ACS APPLIED MATERIALS & INTERFACES

Article

Specific Recognition of Human Influenza Virus with PEDOT Bearing Sialic Acid-Terminated Trisaccharides

Wenfeng Hai, Tatsuro Goda, Hiroaki Takeuchi, Shoji Yamaoka, Yukichi Horiguchi, Akira Matsumoto, and Yuji Miyahara

ACS Appl. Mater. Interfaces, **Just Accepted Manuscript** • DOI: 10.1021/acsami.7b02523 • Publication Date (Web): 05 Apr 2017

ACS Publications

ACS Applied Materials & Interfaces is published by the American Chemical Society. 1155 Sixteenth Street N.W., Washington, DC 20036

Specific Recognition of Human Influenza Virus with PEDOT Bearing Sialic Acid-Terminated Trisaccharides

Wenfeng Hai,[†] Tatsuro Goda,*[,†] Hiroaki Takeuchi,[‡] Shoji Yamaoka,[‡] Yukichi Horiguchi,[†] Akira Matsumoto,[†] and Yuji Miyahara*[,†]

[†] Institute of Biomaterials and Bioengineering, Tokyo Medical and Dental University (TMDU), 2-3-10 Kanda-Surugadai, Chiyoda, Tokyo 101-0062, Japan

[‡] Department of Molecular Virology, Tokyo Medical and Dental University (TMDU), 1-5-45 Yushima, Bunkyo, Tokyo 113-8510, Japan

KEYWORDS: *PEDOT, influenza virus, glycosylation, recognition, impedance, QCM, potentiometry*

ABSTRACT: Conducting polymers are good candidates for biosensor applications when molecular recognition element is imparted. We developed trisaccharide-grafted conducting polymers for label-free detection of the human influenza A virus (H1N1) with high sensitivity and specificity. A 3,4-ethylenedioxythiophene (EDOT) derivative bearing an oxylamine moiety was electrochemically copolymerized with EDOT. The obtained film was characterized by cyclic voltammetry, X-ray photoelectron spectroscopy, scanning electron microscopy, stylus surface profilometer, and AC-impedance spectroscopy. The trisaccharides comprising Sia-α2,6'-Lac-Glu (2,6-sialyllactose) or Sia-α2,3'-Lac-Glu (2,3-sialyllactose) were covalently introduced to the side chain of the conducting polymers as a ligand for viral recognition. Immobilization of sialyllactose was confirmed by quartz crystal microbalance (QCM) and water contact angle measurements. Specific interaction of 2,6-sialyllactose with hemagglutinin in the envelope of the human influenza A virus (H1N1) was detected by QCM and potentiometry with enhanced sensitivity by two orders of magnitude when compared with that of commercially available kits. The developed conducting polymers possessing specific virus recognition are a good candidate material for wearable monitoring and point-of-care testing because of their processability and mass productivity in combination with printing technologies.

1. INTRODUCTION

There is growing interest in the use of conducting polymers, such as poly(3,4-ethylenethiophene (EDOT)) (PEDOT), for biosensors and bioelectronics.[1-6] Conducting polymers have several advantages over inorganic counterparts at biotic/abiotic interfaces, including the ability to conduct both electrical and ionic carriers, mechanical flexibility, low-cytotoxicity,[7-8] low-cost production by casting or printing, and tunable properties via chemical synthesis or doping.[2] The combined electrical and ionic conductivity enable the transduction of ionic input to electrical output and vice versa. PEDOT has been used as an electrode for biosensing because the PEDOT-based electrodes show low impedance when used in biological environments.[3-6] The interaction between biosystems and conducting polymers is not limited to the surface because the hydration of conducting polymers facilitates ion flux that flows into and out of the bulk phase of conducting polymers. This behavior enhances the effective electrochemical surface area of the electrodes. These features minimize interfacial impedance and consequently improve the sensitivity for recording and stimulation.[9-11]

Bioactive molecules such as proteins and polysaccharides can be incorporated or doped into conducting polymers for controlling cell adhesion, cell growth,[12-14] protein adsorption,[15] and other biomolecular recognitions.[16-22] For a low-molecular-weight bioactive dopant, the control of the doping amount over time is difficult because small molecules are typically released from the matrix by diffusion or electrical stimulation. A large bioactive dopant can stably reside in the polymer film, but it may alter the surface and bulk properties of the original material. Chemical introduction of bioactive species to the building block of conducting polymers is another choice. EDOT derivatives have a high degree of freedom for introducing functional groups via versatile synthetic methods.[23-27] In addition, the density of a functional group for bioconjugation and the macromolecular structure of the conducting polymer are easily tunable through polymer chemistry. The control of ligand density is critical for material-induced cell signaling and highly sensitive biosensing. Currently, EDOT derivatives bearing target-capturing elements have been developed for detecting DNA, proteins, cancer cells, dopamine, and glucose.[28-32]

In this study, we aimed to detect the human influenza A virus (H1N1) using functionalized PEDOT. Worldwide, seasonal influenza epidemics are estimated to result in about 3 to 5 million cases of severe illness, and about 250 to 500 thousand deaths.[33] Early-stage diagnosis is critical for preventing a pandemic outbreak, because antiviral medication should be used within 48 h after the onset of symptoms.[34] Identification of the subtypes of influenza virus is also important for preventing highly pathogenic infections in humans.[35] Conventional diagnosis, such as RT-PCR, genetic/antigenic sequencing, immuno- chromatographic tests (ICTs), serology, and viral cultures, needs to be improved in terms of assay time, sensitivity, cost efficiency, and the user interface.[33, 36] Hemagglutinin (HA) is a homotrimeric transmembrane

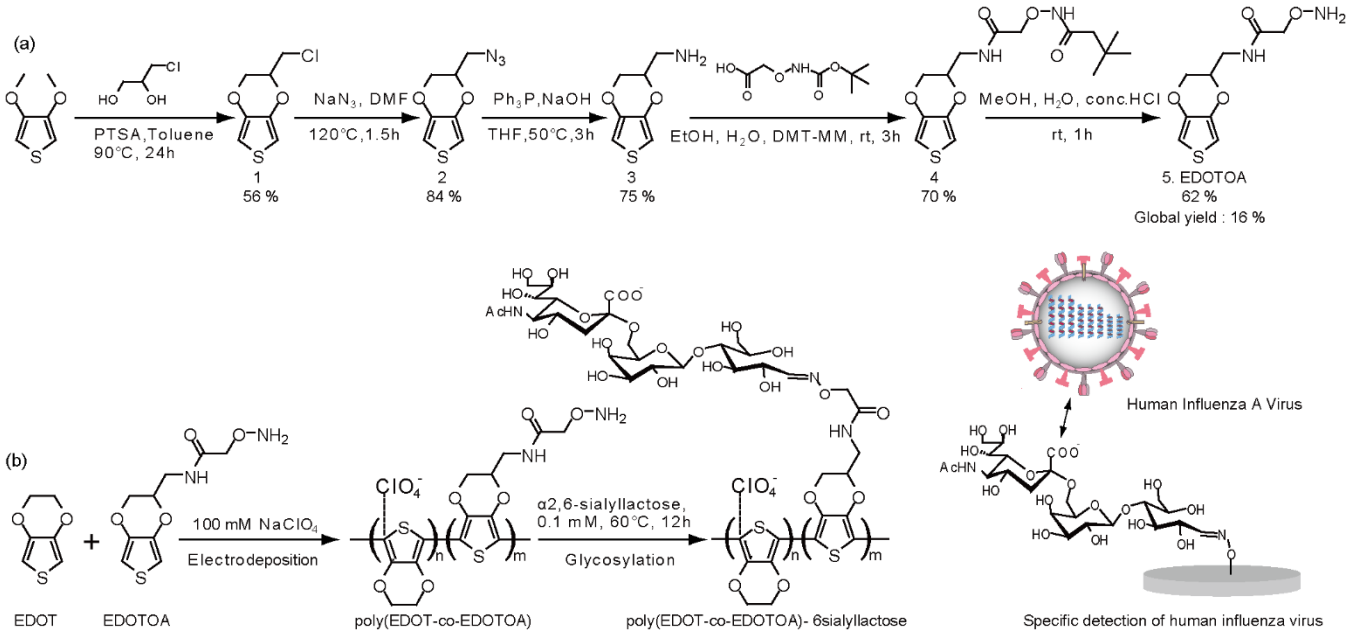

Figure 1. Sialyllactose-grafted polythiophenes for the human influenza A virus (H1N1) detection. (a) Synthetic route of an EDOT derivative possessing an aminooxyl group (EDOTOA). Reaction yield for each step was shown in mol%. (b) Electrochemical copolymerization of EDOT with EDOTOA in the presence of $NaClO_4$ on a glassy carbon electrode followed by glycosylation of an EDOTOA unit with sialyllactose.

glycoprotein expressed on the envelope of influenza virus and binds to sialic acid (SA)-terminated trisaccharides on the epidermal cell membranes for cytoplasmic invasion.[37-38] HA specifically recognizes the linkage between SA and galactose residues in host cell receptors. Human influenza A viruses (H1N1) selectively bind to SA with galactose by α2,6 linkages (2,6-sialyllactose), whereas avian influenza virus binds to SA with galactose by α2,3 linkages (2,3-sialyllactose).[37] Based on this specificity, we have successfully distinguished whole influenza A virus for human from avian.[39] Here, we aimed to develop a new PEDOT derivative bearing 2,6-sialyllactose as a selective ligand for human influenza A virus (H1N1). First, an EDOT bearing oxylamine group (EDOTOA) was synthesized and, then, EDOTOA was electrochemically copolymerized with EDOT under optimized conditions. Then, sialyllactose was chemically introduced to the side chain of the electrodeposited conducting copolymer films by glycosylation as the virus recognition element. Selective interaction of 2,6-sialyllactose with HA on the viral surface was investigated by quartz crystal microbalance (QCM) and potentiometry.

2. RESULTS AND DISCUSSION

2.1. Preparation and Characterization of Poly(EDOT-co-EDOTOA) Films. We developed sialyllactose-grafted PEDOT for capturing human influenza A virus (H1N1). An EDOTOA was synthesized by a five-step reaction with a global yield of 16% (Figure 1a, Figure S1-S2). EDOTOA served as a unit for covalently introducing sialyllactose on the side chain of poly(EDOT-co-EDOTOA) via glycosylation.[40] EDOT and EDOTOA were randomly electrocopolymerized at an arbitrary proportion on an electrode in the presence of the dopant $NaClO_4$ in aqueous solution. We conducted label-free sensing of model human influenza A virus from chicken egg cultures through the specific interaction between the 2,6-sialyllactose-grafted poly(EDOT-co-EDOTOA) and HA expressed on the envelope of human influenza A virus (H1N1) (Figure 1b).

The oxidation potential was observed at +1.0 V during electropolymerization in cyclic voltammetry (CV) (Figure 2a-b). Continuous increases in the cathodic and anodic currents over the CV cycles were observed for 0 and 25 mol% EDOTOA in feed, indicating successful electrodeposition of the conductive polymers on a working electrode.[31, 41] The double layer capacitance at the conducting polymer/solution interface was determined by the difference of forward and backward currents (ΔI) at +0.2 V as follows:

$$C = \Delta I / vA \qquad (1)$$

where v and A are the scan rate and surface area of the electrode, respectively. The capacitance increased by CV cycles at 0 and 25 mol% EDOTOA (Figure 2f). In contrast, almost no changes in the capacitance were observed at 50–100 mol% EDOTOA in feed. The average step height (ASH) and arithmetic average of surface roughness (R_a) of the resultant films decreased by increasing the EDOTOA proportions (Figure 2g-l). The surface morphology of electropolymerized films as determined by scanning electron microscopy (SEM) observations confirmed that the films prepared at 0, 25, 50, and 75 mol % EDOTOA were composed of small particles that formed a rough surface topography (Figure S3). The surface topography of the film prepared at 100 mol% EDOTOA was similar to the surface of the original gold electrode. The low capacitance of the films prepared at 50 and 75 mol% EDOTOA suggests the formation of high-impedance films. The suppression of electropolymerization at 100 mol% EDOTOA may originate from two possibilities: (i) the conformational disorder of π-electron conjugation in the polythiophene main chain is induced by the OA group in the side chain; and (ii) EDOTOA is difficult to deposit on electrode surfaces because of its high solubility in water.

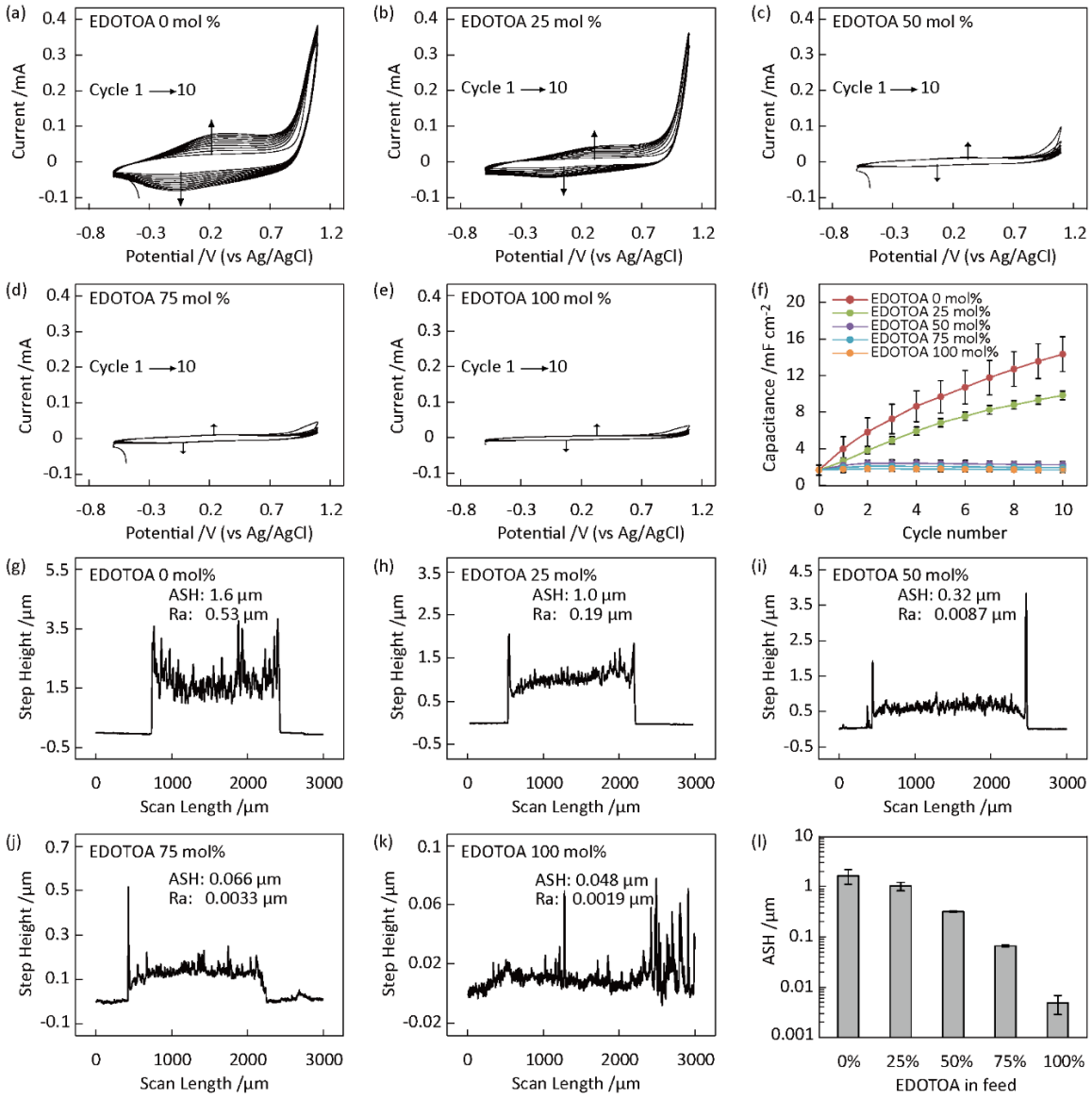

Figure 2. Changes in the capacitance and film thickness by electropolymerization at varying EDOTOA proportions. (a–e) Successive cyclic voltammograms of a glassy carbon electrode in 10 mmol L^{-1} aqueous monomer solutions containing EDOT and EDOTOA at 0 (a), 25 (b), 50 (c), 75 (d), and 100 mol % (e) EDOTOA in feed in the presence of 100 mmol L^{-1} $NaClO_4$. Counter electrode: Pt. Reference electrode: Ag/AgCl (in 3.3 mol L^{-1} KCl with a salt bridge). Scan rate: 0.1 V s^{-1}. (f) Increases in the interface capacitance over the CV cycles at different given EDOTOA proportions. Data are shown as mean ± SD (n = 3). (g–k) Cross section height profiles for the conducting polymer films deposited by 10 CV cycles on a planar electrode at 0 (g), 25 (h), 50 (i), 75 (j), and 100 (k) mol % EDOTOA with 100 mmol L^{-1} NaClO4. (l) An average step height as a function of a given EDOTOA proportion. Mean ± SD (n = 3).

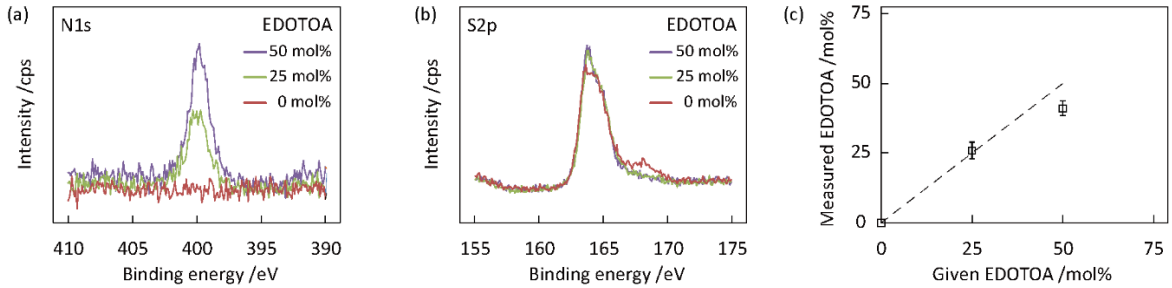

Figure 3. Elemental analysis on the surface of the conducting polymer films. (a,b) High resolution XPS spectra of (a) N1s and (b) S2p of poly (EDOT-co-EDOTOA) films at 0, 25, and 50 mol% EDOTOA in the presence of 100 mmol L^{-1} $NaClO_4$. (c) Comparison of given and measured compositions of EDOTOA in the poly(EDOT-co-EDOTOA) films as determined by the atomic compositions of nitrogen and sulfur as *N/2S*. The dashed line shows stoichiometric conditions.

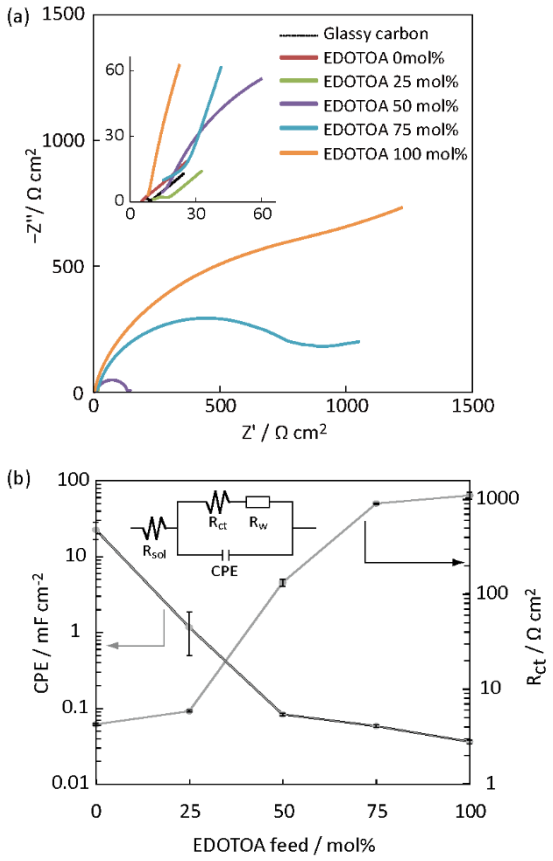

Figure 4. EIS of conducting copolymer films on glassy carbon electrodes. (a) Nyquist plots at the given EDOTOA proportions of conducting copolymers. Inset: A closer view of Nyquist plots at the origin. (b) Changes in the CPE and R_{ct} in the Randle's equivalent circuit model (inset) as a function of a given EDOTOA proportion. Mean ± SD (n = 4).

The N1s peak at the 399 eV in X-ray photoelectron spectroscopy (XPS) confirmed the existence of the EDOTOA unit in the copolymer films (Figure 3a). The peak intensity increased with increasing feed EDOTOA proportion s. In contrast, the S2p peak was not affected by the EDOTOA proportion (Figure 3b). The surface EDOTOA proportions were calculated from the atomic ratios of N and S as N/2S (Figure 3c, supporting information). The measured EDOTOA proportion was equal to the theoretical values at 25 mol% EDOTOA, but it was lower than the theoretical value at 50 mol%. We suggest that the hydrophilic oxylamine moiety is buried in the bulk phase of the copolymer films under high vacuum conditions during the XPS measurement.[42-43] The presence of the EDOTOA unit was also confirmed by attenuated total reflection Fourier transform infrared spectroscopy (ATR-FTIR) (Figure S4).

Low impedance at the solid/liquid interface is important for sensitive biosensing.[9] Therefore, electrochemical impedance spectroscopy (EIS) was conducted for the poly(EDOT-co-EDOTOA) films electrodeposited on a glassy carbon electrode in the presence of 5 mmol L^{-1} $Fe(CN)_6^{3-/4-}$ (Figure 4a). A semicircular part at the high frequencies in the Nyquist plot was dominated by charge transfer of electrons/ions near the conducting polymer surface or bulk, and a linear part at low frequencies corresponded to the diffusion-limited process of the redox couple. Therefore, the Nyquist plots were modeled by the Randle's equivalent circuit.[44] Charge transfer resistance (R_{ct}), which reflects the charge transfer at the conducting polymer/electrolyte interface, increased with an increase in a given EDOTOA proportion (Figure 4b). The constant phase element (CPE), which denotes the double-layer capacitance for a rough surface, decreased with an increase in a given EDOTOA proportion. Trends in the CPE as a function of EDOTOA contents were similar to the interface capacitance determined by CV (Figure 2f). An increase in R_{ct} with the EDOTOA proportion suggests conformational disorder and steric hindrance of the polythiophene main chain exists due to the presence of the oxylamine group. Since the increase in the EDOTOA proportion hindered the charge transfer at the polymer/electrolyte interface, we chose the proportion at 25 mol % EDOTOA for the subsequent glycosylation and human influenza A virus biosensing.

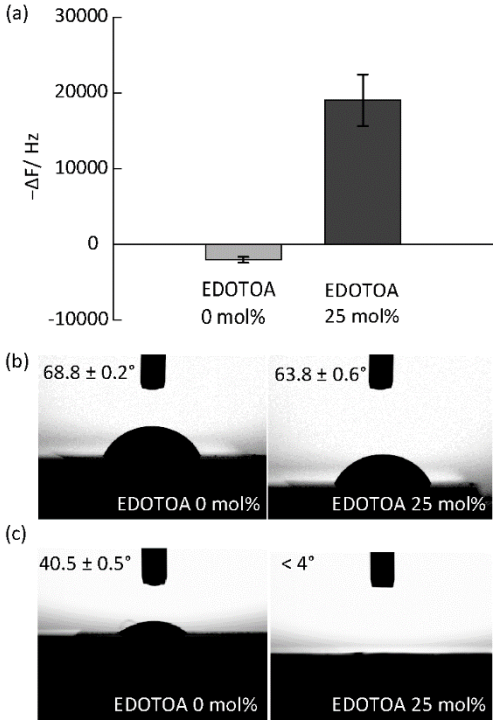

Figure 5. Changes in the surface mass and wettability of the oxylamine-functionalized PEDOT as a result of glycosylation of 2,6-sialyllactose. (a) Changes in the resonance frequency ($-\Delta F$) of QCM in air by glycosylation of poly(EDOT-co-EDOTOA) films at 0 and 25 mol% EDOTOA. (b-c) Static water contact angles of poly(EDOT-co-EDOTOA) films at 0 and 25 mol% EDOTOA before (b) and after (c) glycosylation.

2.2. Glycosylation of Poly(EDOT-co-EDOTOA). A trisaccharide terminating in 2,6-sialyllactose was covalently introduced by glycosylation between the reducing end of lactose and the oxylamine unit in poly(EDOT-co-EDOTOA).[39-40] The glycoblotting was confirmed by changes in the surface mass and wettability (Figure 5). The film prepared at 25 mol % EDOTOA showed changes in the resonance frequency of QCM (ΔF) in air by −19000 ± 3400 Hz following glycosylation of 2,6-sialyllactose. By assuming a condition without nonspecific adsorption of sialyllactose, the value corresponded to an increase in the surface mass by 137 ± 25 ng mm^{-2} based on the Sauerbrey equation ($-\Delta m/\Delta F$ = 7.23 pg mm^{-2} Hz^{-1}) and the molecular weight of sialyllactose (Mw = 655.53 g mol^{-1}).[45] Since the surface density of the EDOTOA unit was 240 ± 3 molecules nm^{-2}, the introduction

rate of sialyllactose to the overall EDOTOA unit in the film was about 52 mol%. The film prepared at 0 mol% EDOTOA (i.e., PEDOT) resulted in a slight decrease in the surface mass. This is caused by dedoping of the remaining ClO_4^- from the bulk phase during the immobilization and rinse processes. The static water contact angles decreased from 63.8 ± 0.2° to below 4° after the glycosylation of the film at 25 mol% EDOTOA (Figure 5b-c). The enhanced wettability indicates the formation of a thick hydration layer of sialyllactose on the surface. A decrease in the contact angle from 68.8 ± 0.2° to 40.5 ± 0.5° was observed on the PEDOT film following the glycosylation process. The contact angle change suggests the remaining of 2,6-sialyllactose even after the washing process.

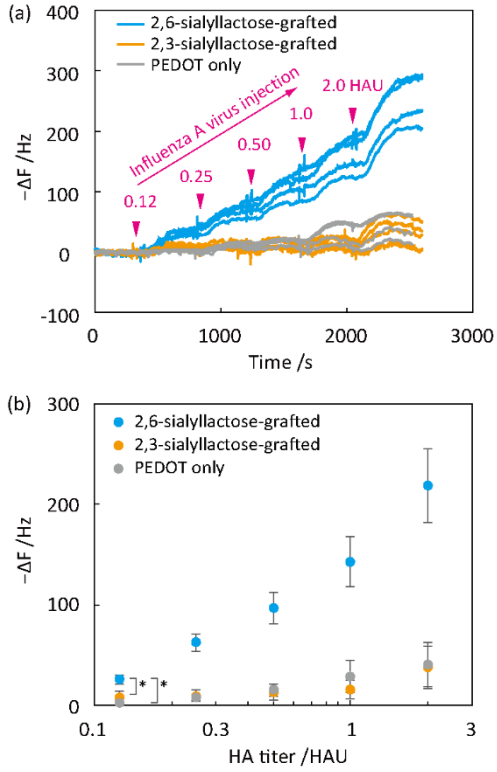

Figure 6. Binding of human influenza A virus (H1N1) on the 2,6-sialyllactose- or 2,3-sialyllactose-grafted poly(EDOT-co-EDOTOA) at 25 mol% EDOTOA in 0.01× DPBS. The surface modified with PEDOT only was used as a control. (a) Time course of QCM signals during sequential injection of the virus solutions with different HAU (0, 0.125, 0.25, 0.5, 1, and 2 HAU) at 25.00 ± 0.02°C. (b) Changes in the resonance frequency as a function of human influenza A virus concentrations from the QCM measurements. Mean ± SD (n = 4). *p < 0.05.

2.3. Binding of Human Influenza A Virus (H1N1) on 2,6-Sialyllactose-Grafted PEDOT. To evaluate the specific recognition of human influenza A virus, QCM measurements were performed on the surface of a sialyllactose-grafted poly(EDOT-co-EDOTOA) film. The original titer of human influenza A virus (H1N1) solution from chicken egg cultures was 256 hemagglutinating units (HAU) (Figure S5). Changes in the resonance frequency (ΔQ) were observed on the 2,6-sialyllactose-immobilized surface at 0.125–2 HAU human influenza A virus (H1N1) (Figure 6a). In contrast, the binding was suppressed on the 2,3-sialyllactose-immobilized surface and PEDOT only surface. Slight changes in the resonance frequency on the 2,3-sialyllactose-modified and PEDOT surfaces at 1–2 HAU were caused by nonspecific adsorption of the virus. The concentration dependence of the QCM signals was analyzed (Figure 6b). The signals on 2,6-sialyllactose-grafted surface were statistically significant ($p < 0.05$) as compared with those on 2,3-sialyllactose-grafted surface and PEDOT only surface at 0.125–2 HAU. In contrast, the signals were statistically insignificant on between the 2,3-sialyllactose-grafted and PEDOT surfaces at 0.125–2 HAU. These results indicate that human influenza A virus (H1N1) specifically recognizes 2,6-sialyllactose on the film. The apparent binding parameters were obtained from the differential signals of 2,6-sialyllactose- and 2,3-sialyllactose- grafted surfaces using the 1:1 Langmuir model (Figure S6). The apparent K_D for human influenza A virus was 0.96 HAU on the 2,6-sialyllactose-immobilized surfaces. The limit of detection (LOD) was 0.12 HAU for QCM. The high affinity is attributed to formation of multiple contacts between HAs on whole human influenza A virus (H1N1) and 2,6-sialyllactose ligands at high surface density.[39] The adsorption amount of human influenza A virus particles per area was 2.3 particles μm^{-2} (Figure S6). Because we used human influenza A virus (H1N1) incubated in a chicken egg culture, the sample solution contained proteins such as ovalbumin and avidins. Therefore, the nonspecific adsorption of these components is not the limiting factor for human influenza A virus sensing on the surface. The reduced nonspecific adsorption was attributed to the thick hydration layer of sialyllactose on the conducting polymer surfaces.

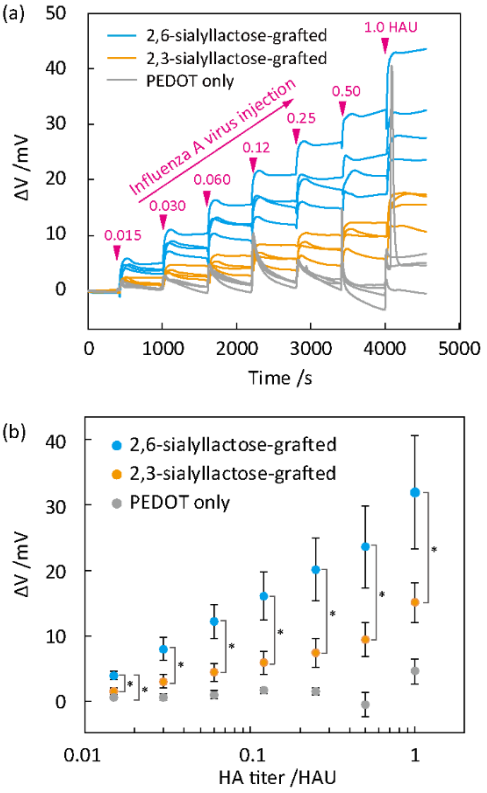

Figure 7. Potentiometric detection of human influenza A virus (H1N1). (a) Time course of the potential change during sequential injection of the human influenza A virus solutions with different HAU (final concentrations: 0, 0.015, 0.03, 0.06, 0.12, 0.25, 0.5 and 1 HAU) in 0.01× DPBS on a 2,6-sialyllactose- or 2,3-sialyllactose-grafted poly(EDOT-co-EDOTOA) film. The electrodes modified with PEDOT only were used as a control. (b) The potential change (ΔV) as a function of human influenza A virus concentrations for each film. Mean ± SD (n = 4). *p < 0.05.

2.4. Label-Free Electrical Sensing of Human Influenza A Virus (H1N1). We extended our study to the label-free electrical detection of human influenza A virus (H1N1) using 2,6-sialyllactose-immobilized conducting polymers. Changes in the open circuit potential as a result of specific binding of the virus were measured (Figure 7a). The potential change (ΔV) increased with increasing HAU on the 2,6-sialyllactose- and 2,3-sialyllactose-grafted electrodes. In contrast, almost no signal changes were obtained on the electrodes modified with PEDOT only at 0.015–0.25 HAU, indicating the requirement of the 2,6-sialyllactose ligand for recognizing human influenza A virus (H1N1). The signals on 2,6-sialyllactose-grafted electrodes were statistically significant ($p < 0.05$) as compared with the signals on 2,3-sialyllactose-grafted and PEDOT-modified electrodes at 0.015–1 HAU (Figure 7b). In contrast, statistically insignificant signals were obtained on between the 2,3-sialyllactose-grafted and PEDOT-modified electrodes at 0.015–1 HAU. The difference in ΔV between the 2,6-sialyllactose and 2,3-sialyllactose surfaces is attributed to the preferential binding of human influenza A virus (H1N1) to 2,6-sialyllactose. We confirmed the binding specificity of 2,6-sialyllactose to HA (H1N1) compared with HA (H5N1) on the poly(EDOT-co-EDOTOA) film at 25 mol% EDOTOA (Figure S7). The apparent K_D and ΔV_{max} were 0.16 HAU and 15.0 mV, respectively, which were determined by the differential signals between the 2,6-sialyllactose- or 2,3-sialyllactose- modified surfaces using the Langmuir equation (Figure S8). The apparent K_D was enhanced in potentiometry as compared with QCM (K_D = 0.96 HAU). The LOD in potentiometry was 0.013 HAU. This is about 2 orders of magnitude better than that of conventional ICT of about 1 HAU and is comparable to other types of influenza virus assays such as surface plasmon resonance (SPR) and ion-sensitive field-effect transistor (ISFET) (Table 1). The potential change (ΔV) was generated by the net-charge change (ΔQ) within the electrical double layer at the electrode/solution interface following the binding event:

$$\Delta V = \Delta Q / C_{int} \quad (2)$$

where C_{int} represents the interface capacitance. Since a diluted Dulbecco's phosphate buffered saline (DPBS) by 100 times with water was used for potentiometry, the solution Debye length was gained to about 8.1 nm.[46] Positive ΔV on the 2,6-sialyllactose-modified surfaces indicate the detection of positive ΔQ of HA with the Stokes radius of 5.5 nm in the double layer at pH 7.4[40, 47-48] because HA on the envelope of influenza A virus accounts for the biomolecular recognition. Positive ΔV was in agreement with the results on potentiometric detection of HA (H1N1 and H5N1) on the 2,6-sialyllactose grafted poly(EDOT-co-EDOTOA) (Figure S7). When C_{int} is not altered by the adsorption event, ΔV is proportional to ΔQ.[46] Because ΔQ is the sum of the net-charges of each HA present on the envelope of human influenza A virus, ΔQ represents the amount of human influenza A virus adsorbed. ΔV on the 2,3-sialyllactose-modified surface were relatively large compared to the QCM results. A possible reason for the high ΔV values on the 2,3-sialyllactose-modified surface is that the charged state of HA depends on the solution pH and ionic strength.[49] The signal on 2,3-sialyllactose-grafted surfaces could be suppressed by optimizing the electrolyte conditions. Another possibility is changes in capacitance as well as charge as a result of the virus adsorption with a small amount onto the 2,3-sialyllactose layer. In our previous report, a mechanism of capacitance change-induced potentiometric signal is proposed on a stimuli-responsive gel-modified surface.[50-51] The above explanation is in accord with insignificant ΔV on PEDOT in the absence of sialyllactose layer (Figure 7b). Although the signal ratio on between 2,6-sialyllactose- and 2,3-sialyllactose-modified surfaces was lower in potentiometry than QCM, potentiometric detection is attractive because it is a straightforward route to the development of point-of-care devices when compared with QCM detection.

3. CONCLUSIONS

We performed sensitive, specific, and label-free biosensing of whole human influenza A virus (H1N1) for humans using PEDOTs functionalized with SA-terminated lactose. EDOTOA was developed for chemical introduction of the sialyllactose. Electrochemical copolymerization under optimized conditions resulted in low impedance at the interface. Specific interaction of 2,6-sialyllactose with HA in the envelope of human influenza A virus (H1N1) allowed label-free sensing by QCM and potentiometry with enhanced sensitivity by a few orders of magnitude when compared with that of commercial kits. Owing to the processability and mass productivity, the conducting polymers developed may find applications in wearable monitoring and point-of-care testing of influenza viruses.

Table 1. Sensing of whole Influenza virus or HA in the literature

Sensor	Sample	Ligand	Sensitivity	Ref.
SPR	A Virus H1N1	Sialyllactose	4.5 pmol L^{-1}	52
ICT*	A Virus (H1N1)	Antibody	1.13 HAU	53
QCM	H5N1 HA	Aptamer	0.0128 HAU	54
Colorimetry	B Virus	SA	512 HAU	55
Impedance	A Virus (H5N1)	Antibody	0.5 HAU	56
ISFET	H1N1 HA H5N1HA	Sialyllactose	5–500 amol L^{-1}	40

4. EXPERIMENTAL SECTION

4.1. Materials. 3,4-dimethoxythiophene, potassium ferricyanide (III), and potassium ferrocyanide (IV) were purchased from Sigma-Aldrich Japan (Tokyo, Japan). 3-chroro-1,2-propanediol, (Boc-aminooxy) acetic acid, 2,3-sialyllactose sodium salt and 2,6-sialyllatose sodium salt were purchased from TCI (Tokyo, Japan). *p*-Toluene sulfonic acid (PTSA) monohydrate, sodium azide (NaN_3), triphenylphosphine (Ph_3P), 4-(4,6-dimethoxy-1,3,5-triazin-2-yl)-4-methylmorphlinium chloride (DMT-MM), sodium perchlorate ($NaClO_4$), DPBS, ethanol (EtOH), and methanol (MeOH) were purchased from Wako Pure Chemicals (Tokyo, Japan). Human influenza A virus (H1N1, A/PR/8/34) was obtained by cultivation in chicken embryos and then detoxified using 0.05% formalin solution. All other reagents of extra pure grade were purchased from commercial sources and were used without further purifications. Milli-Q water (EMD Millipore, Billerica, MA) was used throughout the study.

4.2. Synthesis of EDOTOA. EDOTOA was synthesized by a five-step reaction (Figure 1).[24-25, 57] First, under a nitrogen atmosphere, toluene (28 mL), 3,4-dimethoxythiphene (1.36 g, 10.4 mmol), 3-chloro-1,2-propanediol (2.60 g, 23.1 mmol), and *p*-toluene sulfonic acid monohydrate (0.16 g, 0.92 mmol) were added to a two-neck flask. The mixture was reacted at 90°C for 24 h. Thereafter, another 3-chloro-1,2-propanediol (2.60 g, 23.1 mmol)

was added, and the solution was reacted at 90°C for an additional 3 h. After evaporation of toluene, the residue was purified by column chromatography (silica gel, hexane/dichloromethane = 8/2 v/v) to give 2-(chloromethyl)-2,3-dihydrothieno[3,4-*b*][1,4]dioxine (EDOT-Cl) **1** in yellow oil (yield 56%). Second, *N,N*-dimethylformamide (DMF, 30 mL), EDOT- Cl **1** (1.18 g, 6.18 mmol), and sodium azide (0.48 g, 7.4 mmol) were added to a flask. The mixture was refluxed at 120°C for 1.5 h. After cooling to room temperature, water (15 mL) was added to the solution to extract three times with ethyl acetate (15 mL). The combined organic phase was further washed three times with water, and was dried over anhydrous magnesium sulfate. The collected product was evaporated to give 2-(azidomethyl)-2,3-dihydrothieno[3,4-*b*][1,4]dioxine (EDOT-N_3) **2** in brown oil (yield 81%). Third, tetrahydrofuran (THF) (10 mL), EDOT-N_3 **2** (0.99 g, 5.1 mmol), triphenylphosphine (1.6 g, 6.1 mmol), and 2 M sodium hydroxide aqueous solution (10 mL) were mixed in a two-neck flask and the solution was reacted at 50°C for 3 h. After cooling down to room temperature, the solution was adjusted to an acidic pH (pH < 2) with 1 mol L^{-1} hydrochloric acid aqueous solution. The solution was evaporated to remove THF. The product was washed three times with dichloromethane (15 mL) by discarding the combined organic phases. The aqueous phase was adjusted to alkaline pH (pH > 12) with 1 mol L^{-1} sodium hydroxide aqueous solution. The product was extracted three times with dichloromethane (15 mL). The combined organic phase was dried over anhydrous magnesium sulfate, filtered, and evaporated to obtain (2,3-dihydrothieno[3,4-*b*][1,4]dioxin-2-yl)methanamine (EDOT-NH_2) **3** as yellow oil (yield 75%). Fourth, EDOT-NH_2 **3** (0.65 g, 3.8 mmol), 2-((*tert*-butoxycarbnyl)aminooxy)acetic acid (0.80 g, 4.2 mmol), water (7 mL), and ethanol (13 mL) were mixed in a two-neck flask at room temperature for 10 min. Then, 4-(4,6-dimethoxy-1,3,5-triazin-2-yl)-4-methylmorphlinium chloride (DMT-MM) (1.6 g, 5.7 mmol) was added to the mixture and the reaction was proceeded for 3 h. After evaporation, saturated Na_2CO_3 aqueous solution (15 mL) were added and the mixtures were extracted three times with diethyl ether (15 mL). The organic phase was washed three times with 1 M hydrochloric acid aqueous solution (15 mL), dried over anhydrous sodium sulfate, filtered, and evaporated to obtain *tert*-butyl(2-(((2,3-dihydrothieno[3,4-*b*][1,4]dioxin-2-yl)methyl)amino)-2-oxoethoxy)cabamate (EDOTOA-Boc) **4** as a colorless oil (yield 70%). Finally, EDOTOA-Boc **4** (0.46 g, 1.33 mmol) was dissolved in a mixture of water/methanol (1/3 v/v, 15 mL). While stirring the mixtures, concentrated hydrochloric acid was gradually added. The reaction proceeded for 1 h at room temperature. After adding water (20 mL), the solution was evaporated to remove methanol. The mixture was extracted three times with diethyl ether (15 mL). The aqueous phase was adjusted to alkaline pH (pH > 12) with a 5 mol L^{-1} sodium hydroxide aqueous solution. Then, the solution was extracted three times with diethyl ether (15 mL). The organic phase was dried over anhydrous potassium sulfate and evaporated to obtain 2-(amiooxy)-*N*-((2,3-dihydrothieno[3,4-*b*][1,4]dioxin-2-yl)methyl)acetamide (EDOTOA) **5** as a colorless oil (yield 62%). ^{1}H-NMR (500 MHz in $CDCl_3$, Bruker) and ESI-MS (Bruker Daltonics microTOF-2focus) data were provided in the Supporting Information.

4.3. Electropolymerization. A glassy carbon electrode (inner diameter 3 mm, CH Instruments, Austin, TX) was polished with alumina powder (0.05 μm in grain size, Baikowski International, Charlotte, NC) and washed with water prior to use. EDOT and EDOTOA were added (10 mmol L^{-1} in total) to degassed water (1 mL) containing 100 mmol L^{-1} sodium perchlorate ($NaClO_4$) in a glass cell. A glassy carbon working electrode, a platinum disc counter electrode, and an Ag/AgCl reference electrode (in 3.3 mol L^{-1} KCl via salt bridge) were placed in the cell with connection to Versa STAT 3 potentiostat (Princetfon Applied Research, Oak Ridge, TN). For electropolymerization, cyclic voltammetry (CV) was performed at the potential window from −0.6 to +1.1 to −0.6 V for successive 10 cycles at a scan rate of 0.1 V sec^{-1} and at room temperature. The mean and SD were obtained from three independent measurements.

4.4. Characterization. SEM images were taken using a S-3400N (Hitachi, Tokyo, Japan) at an accelerating voltage of 10 kV, a deceleration voltage of 0 V, a working distance of 9800 μm, and an emission current of 86 μA. Samples were prepared by electropolymerization onto a sputtered gold electrode on a planar quartz substrate and treated by a carbon coater prior to the measurements.

XPS was performed to determine elemental compositions of the films electropolymerized on gold using an AXIS-HSi165 (Shimadzu-Kratos, Kyoto, Japan) equipped with a 15 kV Mg-Kα radiation source at the anode. The take-off angle of the photoelectrons was set at 90°. The curve fitting of the high-resolution spectra was performed by Gaussian functions. The mean and SD were obtained from five measurements at four different positions.

The thickness of the electropolymerized film was measured on a planar gold electrode on a quartz substrate using a Dektak 150 Profilometer (Veeco, Plainview, NY). The mean and SD were obtained at three positions.

Water contact angles on electropolymerized films were measured by the sessile drop method using a DM-501 goniometer (Kyowa Interface Science, Saitama, Japan). The water droplet sizes were 1.0 μL. Mean and SD values were obtained from four independent measurements.

EIS was conducted using a PGSTAT302 potentiostat (Metrohm Autolab, Utrecht, The Netherlands) with a conducting polymer-deposited glassy carbon working electrode by electropolymerization, an Ag/AgCl reference electrode (in 3.3 mol L^{-1} KCl aqueous solution via salt bridge), and a platinum disc counter electrode in the 0.01× DPBS (pH 7.4) containing 5 mmol L^{-1} ferricyanide/ferrocyanide at the frequency range of 0.1 Hz to 10 kHz (10 points per decade) with a 50 mV-AC voltage superimposed on a DC bias of +0.2 V. R_{ct} was determined by fitting the Nyquist plots to the Randle's equivalent circuit. The mean and SD were obtained from four independent measurements.

4.5. Glycosylation of Poly(EDOT-co-EDOTOA). 2,6-sialyllactose (Siaα2,6'Lac) or 2,3-sialyllactose (Siaα2,3'Lac) (100 μmol L^{-1} in acetic acid, pH 5.3) was allowed to react with the EDOTOA unit of conducting polymers in 0.01× DPBS at 60°C for 12 h. The amount of trisaccharides immobilized on the poly(EDOT-co-EDOTOA) films at 25 mol% EDOTOA was measured using a NAPiCOS QCM twin sensor (Nihon Dempa Kogyo, Tokyo Japan) at the fundamental frequency of 30 MHz at 25.00 ± 0.02°C. The mean and SD were obtained from three independent measurements.

4.6. QCM Sensing of Human Influenza A Virus (H1N1). The amount of human influenza A virus (H1N1) adsorbed on the 2,6-

sialyllatose- or 2,3-sialyllatose- grafted poly(EDOT-co-EDOTOA) at 25 mol% EDOTOA was determined by QCM. The gold surface modified with poly(EDOT-co-EDOTOA) at 0 mol% EDOTOA (i.e., PEDOT) were used as a control. The binding experiments were performed by injecting 200-μL human influenza A virus (H1N1) in 0.01× DPBS with 2 times dilution series (0.125–2 HAU) at 7-min intervals and a flow rate of 3 mL h^{-1} using a syringe pump at 25.00 ± 0.02°C. The mean and SD were obtained from three independent measurements. The LOD was defined as the HAU that is equivalent to three-times the value of the SD for the differential QCM signal between 2,6-sialyllatose- and 2,3-sialyllactose- modified surfaces. The data were analyzed by ANOVA (one-way), followed by Tukey's test for multiple comparisons. $P < 0.05$ was considered statistically significant.

4.7. Potentiometric Sensing of Human Influenza A Virus (H1N1). Potentiometric detection of human influenza A virus (H1N1) was performed using a 6517B multi-channel high input-impedance electrometer (Keithley Instrument, Cleveland, OH) using 2,6-sialyllatose- or 2,3-sialyllatose- grafted poly(EDOT-co-EDOTOA) at 25 mol% EDOTOA on screen printed circular gold electrodes (0.5 mm in diameter) on a chip as working electrodes at no DC bias from an Ag/AgCl reference electrode (in 3.3 mol L^{-1} KCl with a salt bridge) at room temperature. The gold electrodes modified with poly(EDOT-co-EDOTOA) at 0 mol% EDOTOA (i.e., PEDOT) were used as a control. After stabilizing the potential in 0.01× DPBS for 120 min, a stock solution of human influenza A virus (H1N1) was sequentially added to the measurement solution to give final concentrations of 0.15, 0.3, 0.5, 0.75 and 1 HAU. The mean and SD were obtained from four independent electrodes. The LOD was defined as the HAU that is equivalent to three-times the value of the SD for the differential potential between 2,6-sialyllatose- and 2,3-sialyllactose- modified electrodes. The data were analyzed by ANOVA (one-way), followed by Tukey's test for multiple comparisons. $P < 0.05$ was considered statistically significant.

ASSOCIATED CONTENT

Supporting Information.

The supporting information is available free of charge on the ACS publications website at DOI: xxx.

NMR and ESI-MS data for EDOTOA; SEM images and ATR-FTTR spectra for poly(EDOT-co-EDOTOA) films; HA titer tests for human influenza A virus; Langmuir isotherm analysis for QCM and potentiometry; Binding specificity of 2,6-sialyllactose to HA on the poly(EDOT-co-EDOTOA) film.

AUTHOR INFORMATION

Corresponding Author

* E-mail: goda.bsr@tmd.ac.jp (T.G.), miyahara.bsr@tmd.ac.jp (Y.M.)

ORCID

Tatsuro Goda: 0000-0003-2688-8186
Yukichi Horiguchi: 0000-0002-6748-9643

Author Contributions

T.G. conceived and designed the experiments. W.H. performed the experiments. W.H. and T.G. analyzed the data. H.T. and S.Y. produced the human influenza A virus. W.H., and T.G. wrote the paper. T.G., Y.H., A.M., and Y.M. supervised the project.

Notes

We declare competing financial interest as follows: Japanese patent application (#PCT/JP2017/001780, submitted: January 19, 2017).

ACKNOWLEDGMENTS

T.G. is grateful for financial support from a Grant-in-Aid for Scientific Research on Innovative Areas (#26107705) from MEXT of Japan, and the Futaba Electronics Foundation. W.H., T.G., Y.H., A.M., and Y.M. acknowledge financial support from the ImPACT Miyata program from the JST agency. We acknowledge Prof. K. Mitsubayashi at TMDU for offering the use of the stylus surface profiler and Prof. K. Ishihara at the University of Tokyo for providing access to a XPS.

REFERENCES

(1) Guo, B. L.; Glavas, L.; Albertsson, A. C., Biodegradable and Electrically Conducting Polymers for Biomedical Applications. *Prog. Polym. Sci.* **2013,** *38*, 1263-1286.

(2) Balint, R.; Cassidy, N. J.; Cartmell, S. H., Conductive polymers: Towards a Smart Biomaterial for Tissue Engineering. *Acta Biomater.* **2014,** *10*, 2341-2353.

(3) Liao, C. Z.; Zhang, M.; Yao, M. Y.; Hua, T.; Li, L.; Yan, F., Flexible Organic Electronics in Biology: Materials and Devices. *Adv. Mater.* **2015,** *27*, 7493-7527.

(4) Simon, D. T.; Gabrielsson, E. O.; Tybrandt, K.; Berggren, M., Organic Bioelectronics: Bridging the Signaling Gap between Biology and Technology. *Chem. Rev.* **2016,** *116*, 13009-13041.

(5) Strakosas, X.; Wei, B.; Martin, D. C.; Owens, R. M., Biofunctionalization of Polydioxythiophene Derivatives for Biomedical Applications. *J. Mater. Chem. B* **2016,** *4*, 4952-4968.

(6) Someya, T.; Bao, Z. N.; Malliaras, G. G., The Rise of Plastic Bioelectronics. *Nature* **2016,** *540*, 379-385.

(7) Luo, S. C.; Ali, E. M.; Tansil, N. C.; Yu, H. H.; Gao, S.; Kantchev, E. A. B.; Ying, J. Y., Poly(3,4-ethylenedioxythiophene) (PEDOT) Nanobiointerfaces: Thin, Ultrasmooth, and Functionalized PEDOT Films with In Vitro and In Vivo Biocompatibility. *Langmuir* **2008,** *24*, 8071-8077.

(8) Rivnay, J.; Owens, R. M.; Malliaras, G. G., The Rise of Organic Bioelectronics. *Chem. Mater.* **2014,** *26*, 679-685.

(9) Wallace, G. G.; Moulton, S. E.; Clark, G. M., Electrode-Cellular Interface. *Science* **2009,** *324*, 185-186.

(10) Sessolo, M.; Khodagholy, D.; Rivnay, J.; Maddalena, F.; Gleyzes, M.; Steidl, E.; Buisson, B.; Malliaras, G. G., Easy-to-Fabricate Conducting Polymer Microelectrode Arrays. *Adv. Mater.* **2013,** *25*, 2135-2139.

(11) Williamson, A.; Rivnay, J.; Kergoat, L.; Jonsson, A.; Inal, S.; Uguz, I.; Ferro, M.; Ivanov, A.; Sjostrom, T. A.; Simon, D. T.; Berggren, M.; Malliaras, G. G.; Bernard, C., Controlling Epileptiform Activity with Organic Electronic Ion Pumps. *Adv. Mater.* **2015,** *27*, 3138-3144.

(12) Green, R. A.; Lovell, N. H.; Poole-Warren, L. A., Cell Attachment Functionality of Bioactive Conducting Polymers for Neural Interfaces. *Biomaterials* **2009,** *30*, 3637-3644.

(13) Marzocchi, M.; Gualandi, I.; Calienni, M.; Zironi, I.; Scavetta, E.; Castellani, G.; Fraboni, B., Physical and Electrochemical Properties of PEDOT:PSS as a Tool for Controlling Cell Growth. *ACS Appl. Mater. Interfaces* **2015,** *7*, 17993-18003.

(14) Mantione, D.; del Agua, I.; Schaafsma, W.; Diez-Garcia, J.; Castro, B.; Sardon, H.; Mecerreyes, D., Poly(3,4-Ethylenedioxythiophene):GlycosAminoGlycan Aqueous Dispersions: Toward Electrically Conductive Bioactive Materials for Neural Interfaces. *Macromol. Biosci.* **2016,** *16*, 1227-1238.

(15) Zhao, H. C.; Zhu, B.; Luo, S. C.; Lin, H. A.; Nakao, A.; Yamashita, Y.; Yu, H. H., Controlled Protein Absorption and Cell Adhesion on Polymer-Brush-Grafted Poly(3,4-ethylenedioxythiophene) Films. *ACS Appl. Mater. Interfaces* **2013,** *5*, 4536-4543.

(16) Arter, J. A.; Taggart, D. K.; McIntire, T. M.; Penner, R. M.; Weiss, G. A., Virus-PEDOT Nanowires for Biosensing. *Nano Lett.* **2010,** *10*, 4858-4862.
(17) Luo, S. C.; Kantchev, E. A.; Zhu, B.; Siang, Y. W.; Yu, H. H., Tunable, Dynamic and Electrically Stimulated Lectin-Carbohydrate Recognition on a Glycan-Grafted Conjugated Polymer. *Chem. Commun. (Cambridge, U. K.)* **2012,** *48*, 6942-6944.
(18) Wen, Y. P.; Xu, J. K.; Li, D.; Liu, M.; Kong, F. F.; He, H. H., A Novel Electrochemical Biosensing Platform Based on Poly(3,4-Ethylenedioxythiophene):Poly(styrenesulfonate) Composites. *Synth. Met.* **2012,** *162*, 1308-1314.
(19) Kergoat, L.; Piro, B.; Simon, D. T.; Pham, M. C.; Noel, V.; Berggren, M., Detection of Glutamate and Acetylcholine with Organic Electrochemical Transistors Based on Conducting Polymer/Platinum Nanoparticle Composites. *Adv. Mater.* **2014,** *26*, 5658-5664.
(20) Chen, C. H.; Luo, S. C., Tuning Surface Charge and Morphology for the Efficient Detection of Dopamine under the Interferences of Uric Acid, Ascorbic Acid, and Protein Adsorption. *ACS Appl. Mater. Interfaces* **2015,** *7*, 21931-21938.
(21) Welch, M. E.; Doublet, T.; Bernard, C.; Malliaras, G. G.; Ober, C. K., A Glucose Sensor via Stable Immobilization of the GOx Enzyme on an Organic Transistor Using a Polymer Brush. *J. Polym. Sci., Part A: Polym. Chem.* **2015,** *53*, 372-377.
(22) Pal, R. K.; Farghaly, A. A.; Wang, C. Z.; Collinson, M. M.; Kundu, S. C.; Yadavalli, V. K., Conducting Polymer-Silk Biocomposites for Flexible and Biodegradable Electrochemical Sensors. *Biosens. Bioelectron.* **2016,** *81*, 294-302.
(23) Groenendaal, B. L.; Jonas, F.; Freitag, D.; Pielartzik, H.; Reynolds, J. R., Poly(3,4-Ethylenedioxythiophene) and its Derivatives: Past, Present, and Future. *Adv. Mater.* **2000,** *12*, 481-494.
(24) Segura, J. L.; Gomez, R.; Blanco, R.; Reinold, E.; Bauerle, P., Synthesis and Electronic Properties of Anthraquinone-, Tetracyanoanthraquinodimethane-, and Perylenetetracarboxylic Diimide-Functionalized Poly(3,4-Ethylenedioxythiophenes). *Chem. Mater.* **2006,** *18*, 2834-2847.
(25) Bu, H. B.; Gotz, G.; Reinold, E.; Vogt, A.; Schmid, S.; Segura, J. L.; Blanco, R.; Gomez, R.; Bauerle, P., Efficient Post-Polymerization Functionalization of Conducting Poly(3,4-Ethylenedioxythiophene) (PEDOT) via 'Click'-Reaction. *Tetrahedron* **2011,** *67*, 1114-1125.
(26) Darmanin, T.; Guittard, F., Superhydrophobic Fiber Mats by Electrodeposition of Fluorinated Poly(3,4-Ethyleneoxythiathiophene). *J. Am. Chem. Soc.* **2011,** *133*, 15627-15634.
(27) Luo, S. C.; Sekine, J.; Zhu, B.; Zhao, H. C.; Nakao, A.; Yu, H. H., Polydioxythiophene Nanodots, Nonowires, Nano-Networks, and Tubular Structures: The Effect of Functional Groups and Temperature in Template-Free Electropolymerization. *ACS Nano* **2012,** *6*, 3018-3026.
(28) Liu, J.; Agarwal, M.; Varahramyan, K., Glucose Sensor based on Organic Thin Film Transistor Using Glucose Oxidase and Conducting Polymer. *Sens. Actuators, B* **2008,** *135*, 195-199.
(29) Tang, H.; Lin, P.; Chan, H. L. W.; Yan, F., Highly Sensitive Dopamine Biosensors based on Organic Electrochemical Transistors. *Biosens. Bioelectron.* **2011,** *26*, 4559-4563.
(30) Galan, T.; Prieto-Simon, B.; Alvira, M.; Eritja, R.; Gotz, G.; Bauerle, P.; Samitier, J., Label-Free Electrochemical DNA Sensor using "Click"-Functionalized PEDOT Electrodes. *Biosens. Bioelectron.* **2015,** *74*, 751-756.
(31) Goda, T.; Toya, M.; Matsumoto, A.; Miyahara, Y., Poly(3,4-ethylenedioxythiophene) Bearing Phosphorylcholine Groups for Metal-Free, Antibody-Free, and Low-Impedance Biosensors Specific for C-Reactive Protein. *ACS Appl. Mater. Interfaces* **2015,** *7*, 27440-27448.
(32) Guo, X.; Liu, J.; Liu, F. Y.; She, F.; Zheng, Q.; Tang, H.; Ma, M.; Yao, S. Z., Label-Free and Sensitive Sialic Acid Biosensor Based on Organic Electrochemical Transistors. *Sens. Actuators, B* **2017,** *240*, 1075-1082.
(33) Vemula, S. V.; Zhao, J. Q.; Liu, J. K.; Wang, X.; Biswas, S.; Hewlett, I., Current Approaches for Diagnosis of Influenza Virus Infections in Humans. *Viruses* **2016,** *8*, 96.
(34) Moscona, A., Drug Therapy - Neuraminidase Inhibitors for Influenza. *N. Engl. J. Med.* **2005,** *353*, 1363-1373.
(35) Subbarao, K.; Klimov, A.; Katz, J.; Regnery, H.; Lim, W.; Hall, H.; Perdue, M.; Swayne, D.; Bender, C.; Huang, J.; Hemphill, M.; Rowe, T.; Shaw, M.; Xu, X. Y.; Fukuda, K.; Cox, N., Characterization of an Avian Influenza A (H5N1) Virus Isolated from a Child with a Fatal Respiratory Illness. *Science* **1998,** *279*, 393-396.
(36) Gopinath, S. C. B.; Tang, T. H.; Chen, Y.; Citartan, M.; Tominaga, J.; Lakshmipriya, T., Sensing Strategies for Influenza Surveillance. *Biosens. Bioelectron.* **2014,** *61*, 357-369.
(37) Skehel, J. J.; Wiley, D. C., Receptor Binding and Membrane Fusion in Virus Entry: The Influenza Hemagglutinin. *Annu. Rev. Biochem.* **2000,** *69*, 531-569.
(38) Medina, R. A.; Garcia-Sastre, A., Influenza A Viruses: New Research Developments. *Nat. Rev. Microbiol.* **2011,** *9*, 590-603.
(39) Horiguchi, Y.; Goda, T.; Matsumoto, A.; Takeuchi, H.; Yamaoka, S.; Miyahara, Y., Direct and Label-Free Influenza Virus Detection Based on Multisite Binding to Sialic Acid Receptors. *Biosens. Bioelectron.* **2017,** *92*, 234-240.
(40) Hideshima, S.; Hinou, H.; Ebihara, D.; Sato, R.; Kuroiwa, S.; Nakanishi, T.; Nishimura, S. I.; Osaka, T., Attomolar Detection of Influenza A Virus Hemagglutinin Human H1 and Avian H5 Using Glycan-Blotted Field Effect Transistor Biosensor. *Anal. Chem.* **2013,** *85*, 5641-5644.
(41) Lapkowski, M.; Pron, A., Electrochemical Oxidation of Poly(3,4-Ethylenedioxythiophene) - "In Situ" Conductivity and Spectroscopic Investigations. *Synthetic Met.* **2000,** *110*, 79-83.
(42) Truica-Marasescu, F.; Jedrzejowski, P.; Wertheimer, M. R., Hydrophobic Recovery of Vacuum Ultraviolet Irradiated Polyolefin Surfaces. *Plasma Processes Polym.* **2004,** *1*, 153-163.
(43) Futamura, K.; Matsuno, R.; Konno, T.; Takai, M.; Ishihara, K., Rapid Development of Hydrophilicity and Protein Adsorption Resistance by Polymer Surfaces Bearing Phosphorylcholine and Naphthalene Groups. *Langmuir* **2008,** *24*, 10340-10344.
(44) Sundfors, F.; Bobacka, J.; Ivaska, A.; Lewenstam, A., Kinetics of Electron Transfer between Fe(CN)(6)(3-/4-) and Poly(3,4-ethylenedioxythiophene) Studied by Electrochemical Impedance Spectroscopy. *Electrochim. Acta* **2002,** *47*, 2245-2251.
(45) Bruckenstein, S.; Shay, M., Experimental Aspects of Use of the Quartz Crystal Microbalance in Solution. *Electrochim. Acta* **1985,** *30*, 1295-1300.
(46) Goda, T.; Miyahara, Y., Interpretation of Protein Adsorption through Its Intrinsic Electric Charges: A Comparative Study Using a Field-Effect Transistor, Surface Plasmon Resonance, and Quartz Crystal Microbalance. *Langmuir* **2012,** *28*, 14730-14738.
(47) Giga, Y.; Sutoh, K.; Ikai, A., A New Multimeric Hemagglutinin from the Coelomic Fluid of the Sea Urchin Anthocidaris Crassispina. *Biochemistry* **1985,** *24*, 4461-4467.
(48) Sawada, T.; Fedorov, D. G.; Kitaura, K., Role of the Key Mutation in the Selective Binding of Avian and Human Influenza Hemagglutinin to Sialosides Revealed by Quantum-Mechanical Calculations. *J. Am. Chem. Soc.* **2010,** *132*, 16862-16872.
(49) Goda, T.; Higashi, D.; Matsumoto, A.; Hoshi, T.; Sawaguchi, T.; Miyahara, Y., Dual Aptamer-Immobilized Surfaces for Improved Affinity through Multiple Target Binding in Potentiometric Thrombin Biosensing. *Biosens. Bioelectron.* **2015,** *73*, 174-180.
(50) Matsumoto, A.; Sato, N.; Sakata, T.; Yoshida, R.; Kataoka, K.; Miyahara, Y., Chemical-to-Electrical-Signal Transduction

Synchronized with Smart Gel Volume Phase Transition. *Adv. Mater.* **2009,** *21*, 4372-4378.
(51) Maeda, Y.; Matsumoto, A.; Miura, Y.; Miyahara, Y., Preparation of alpha-Mannoside Hydrogel and Electrical Detection of Saccharide-Protein Interactions Using the Smart Gel-Modified Gate Field Effect Transistor. *Nanoscale Res. Lett.* **2012,** *7*, 1-8.
(52) Critchley, P.; Dimmock, N. J., Binding of an Influenza A Virus to a Neomembrane Measured by Surface Plasmon Resonance. *Bioorg. Med. Chem.* **2004,** *12*, 2773-2780.
(53) Lee, G. C.; Jeon, E. S.; Kim, W. S.; Le, D. T.; Yoo, J. H.; Chong, C. K., Evaluation of a Rapid Diagnostic Test, NanoSign (R) Influenza A/B Antigen, for Detection of the 2009 Pandemic Influenza A/H1N1 Viruses. *Virol. J.* **2010,** *7*, 244.
(54) Wang, R. H.; Li, Y. B., Hydrogel based QCM Aptasensor for Detection of Avian Influenza Virus. *Biosens. Bioelectron.* **2013,** *42*, 148-155.
(55) Lee, C.; Gaston, M. A.; Weiss, A. A.; Zhang, P., Colorimetric Viral Detection based on Sialic Acid Stabilized Gold Nanoparticles. *Biosens. Bioelectron.* **2013,** *42*, 236-241.
(56) Lin, J. H.; Wang, R. H.; Jiao, P. R.; Li, Y. T.; Li, Y. B.; Liao, M.; Yu, Y. D.; Wang, M. H., An Impedance Immunosensor based on Low-Cost Microelectrodes and Specific Monoclonal Antibodies for Rapid Detection of Avian Influenza Virus H5N1 in Chicken Swabs. *Biosens. Bioelectron.* **2015,** *67*, 546-552.
(57) Maiti, S. N.; Singh, M. P.; Micetich, R. G., Facile Conversion of Azides to Amines. *Tetrahedron Lett.* **1986,** *27*, 1423-1424.

SYNOPSIS TOC (Word Style "SN_Synopsis_TOC").

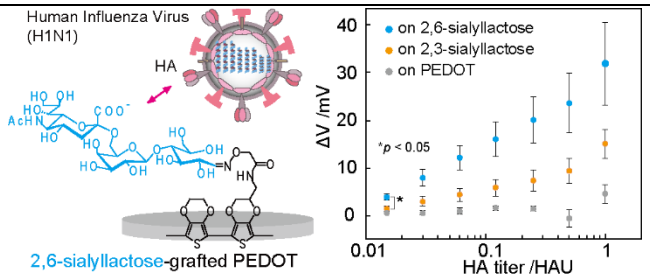

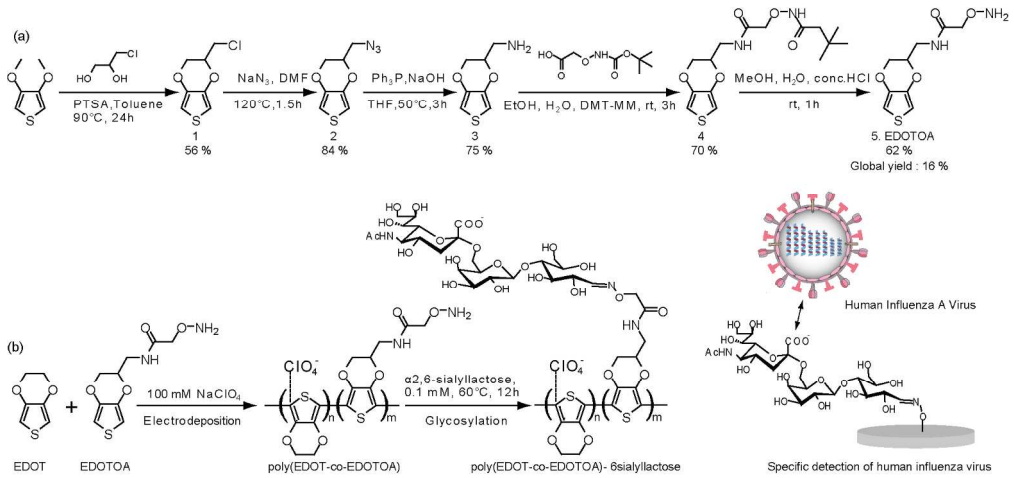

Figure 1. Sialyllactose-grafted polythiophenes for the human influenza A virus (H1N1) detection. (a) Synthetic route of an EDOT derivative possessing an aminooxyl group (EDOTOA). Reaction yield for each step was shown in mol%. (b) Electrochemical copolymerization of EDOT with EDOTOA in the presence of NaClO4 on a glassy carbon electrode followed by glycosylation of an EDOTOA unit with sialyllactose.
Figure 1
179x83mm (300 x 300 DPI)

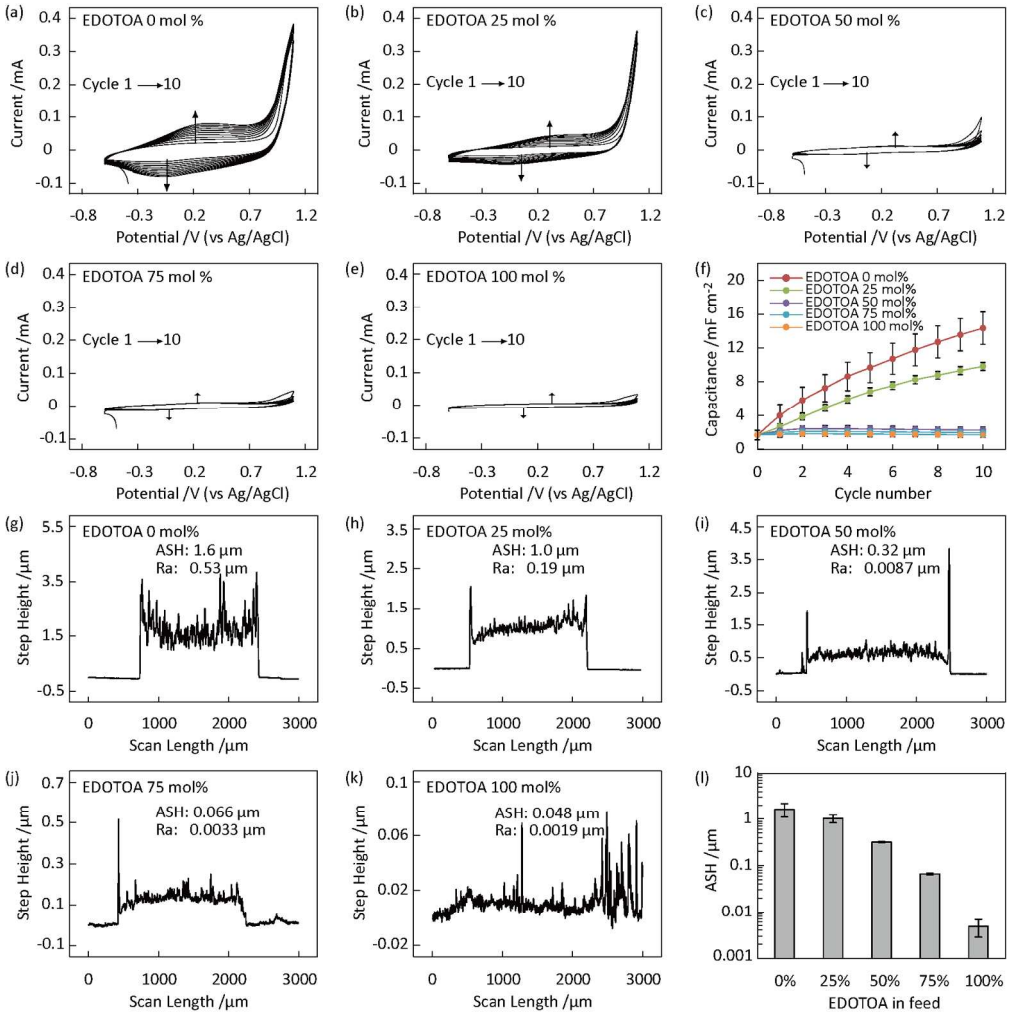

Figure 2. Changes in the capacitance and film thickness by electropolymerization at varying EDOTOA proportions. (a–e) Successive cyclic voltammograms of a glassy carbon electrode in 10 mmol L−1 aqueous monomer solutions containing EDOT and EDOTOA at 0 (a), 25 (b), 50 (c), 75 (d), and 100 mol % (e) EDOTOA in feed in the presence of 100 mmol L−1 NaClO4. Counter electrode: Pt. Reference electrode: Ag/AgCl (in 3.3 mol L−1 KCl with a salt bridge). Scan rate: 0.1 V s−1. (f) Increases in the interface capacitance over the CV cycles at different given EDOTOA proportions. Data are shown as mean ± SD (n = 3). (g–k) Cross section height profiles for the conducting polymer films deposited by 10 CV cycles on a planar electrode at 0 (g), 25 (h), 50 (i), 75 (j), and 100 (k) mol % EDOTOA with 100 mmol L−1 NaClO4. (l) An average step height as a function of a given EDOTOA proportion. Mean ± SD (n = 3).

Figure 2
161x163mm (300 x 300 DPI)

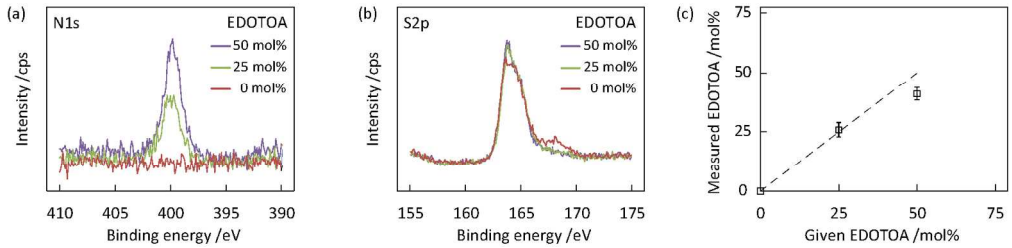

Figure 3. Elemental analysis on the surface of the conducting polymer films. (a,b) High resolution XPS spectra of (a) N1s and (b) S2p of poly (EDOT-co-EDOTOA) films at 0, 25, and 50 mol% EDOTOA in the presence of 100 mmol L−1 NaClO4. (c) Comparison of given and measured compositions of EDOTOA in the poly(EDOT-co-EDOTOA) films as determined by the atomic compositions of nitrogen and sulfur as N/2S. The dashed line shows stoichiometric conditions.
Figure 3
162x39mm (300 x 300 DPI)

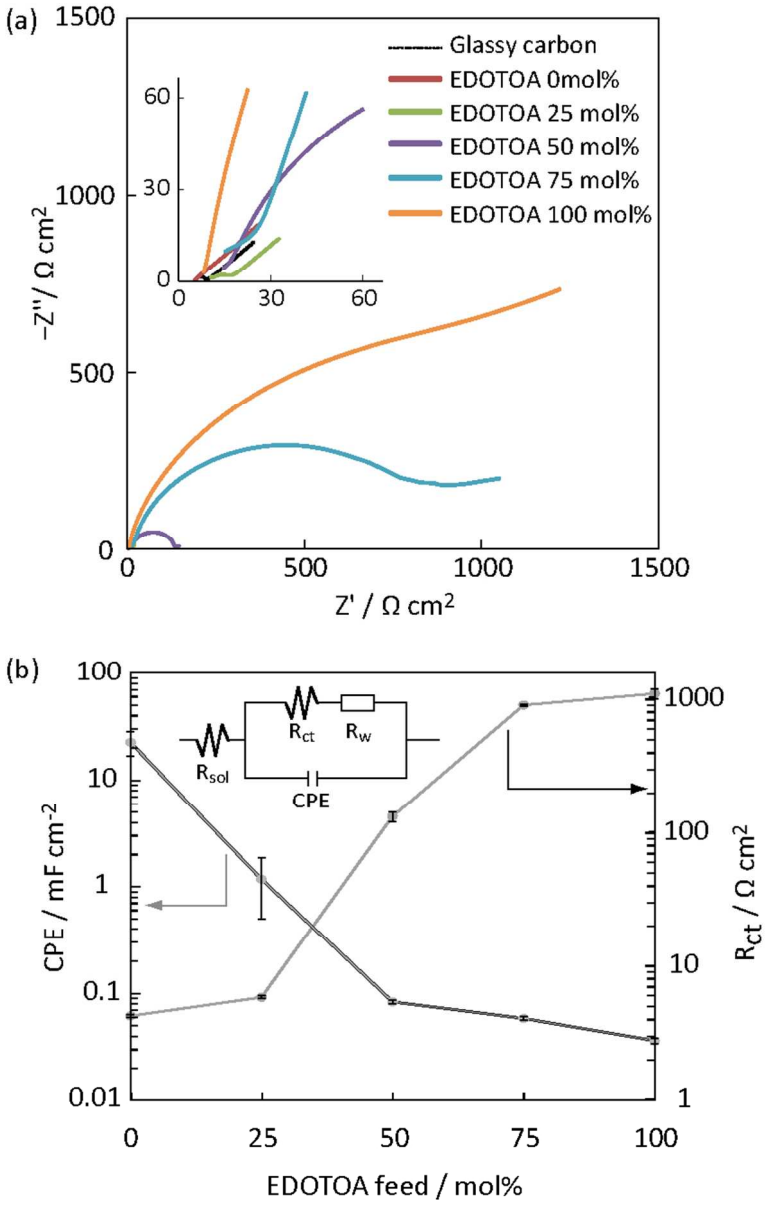

Figure 4. EIS of conducting copolymer films on glassy carbon electrodes. (a) Nyquist plots at the given EDOTOA proportions of conducting copolymers. Inset: A closer view of Nyquist plots at the origin. (b) Changes in the CPE and Rct in the Randle's equivalent circuit model (inset) as a function of a given EDOTOA proportion. Mean ± SD (n = 4).

Figure 4
72x112mm (300 x 300 DPI)

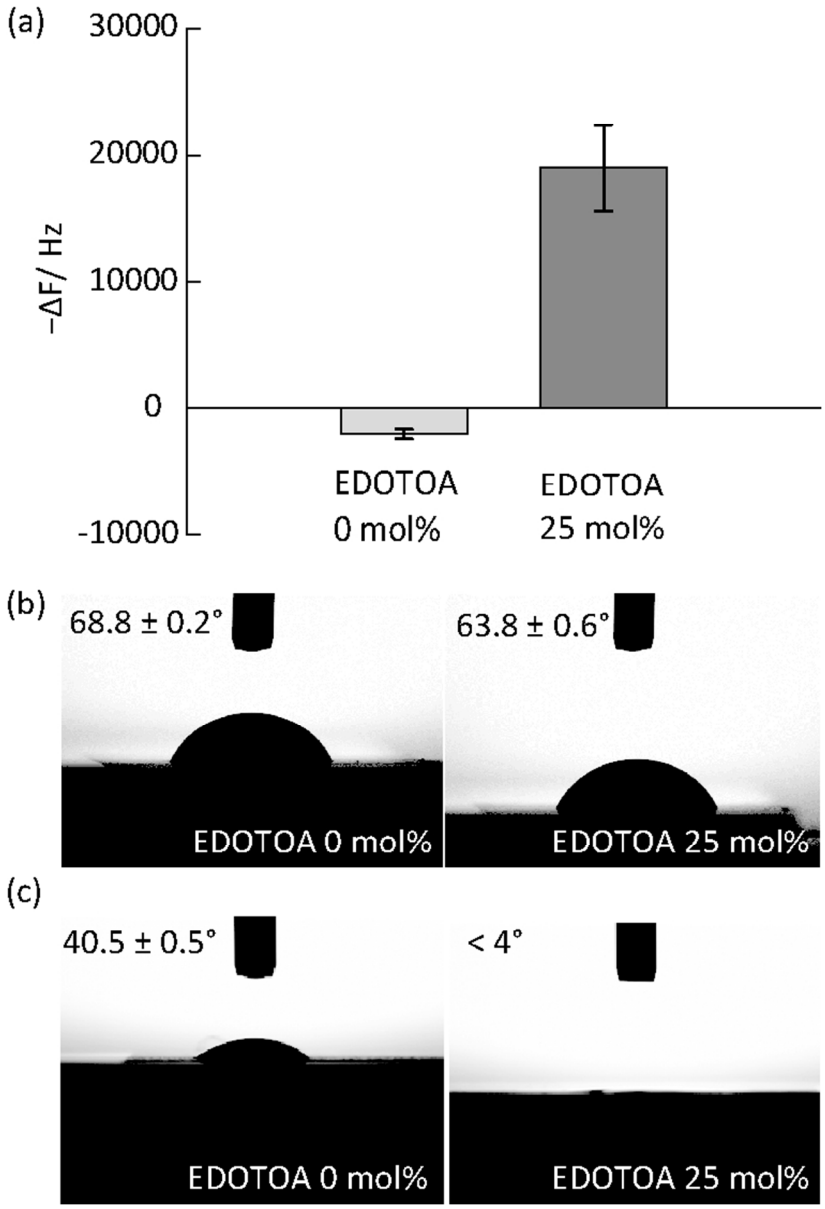

Figure 5. Changes in the surface mass and wettability of the oxylamine-functionalized PEDOT as a result of glycosylation of 2,6-sialyllactose. (a) Changes in the resonance frequency (−ΔF) of QCM in air by glycosylation of poly(EDOT-co-EDOTOA) films at 0 and 25 mol% EDOTOA. (b-c) Static water contact angles of poly(EDOT-co-EDOTOA) films at 0 and 25 mol% EDOTOA before (b) and after (c) glycosylation.
Figure 5
64x94mm (300 x 300 DPI)

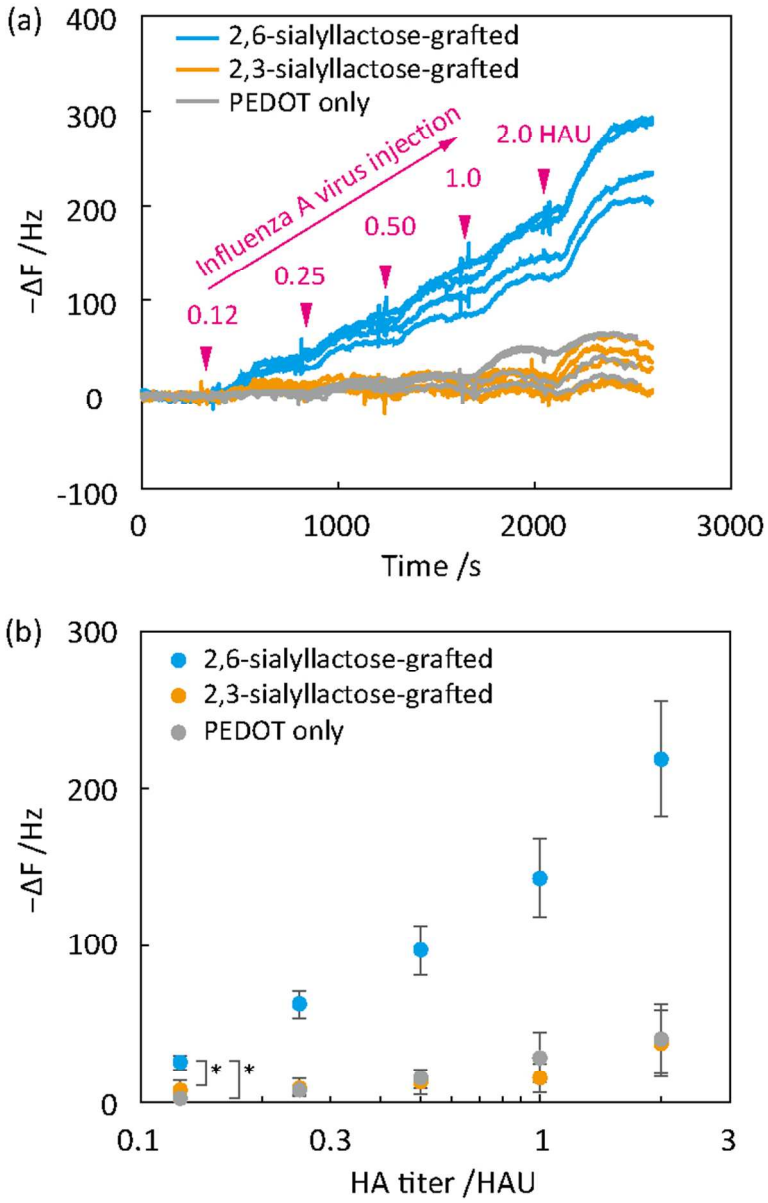

Figure 6. Binding of human influenza A virus (H1N1) on the 2,6-sialyllactose- or 2,3-sialyllactose-grafted poly(EDOT-co-EDOTOA) at 25 mol% EDOTOA in 0.01× DPBS. The surface modified with PEDOT only was used as a control. (a) Time course of QCM signals during sequential injection of the virus solutions with different HAU (0, 0.125, 0.25, 0.5, 1, and 2 HAU) at 25.00 ± 0.02°C. (b) Changes in the resonance frequency as a function of human influenza A virus concentrations from the QCM measurements. Mean ± SD (n = 4). *p < 0.05.

Figure 6
64x101mm (300 x 300 DPI)

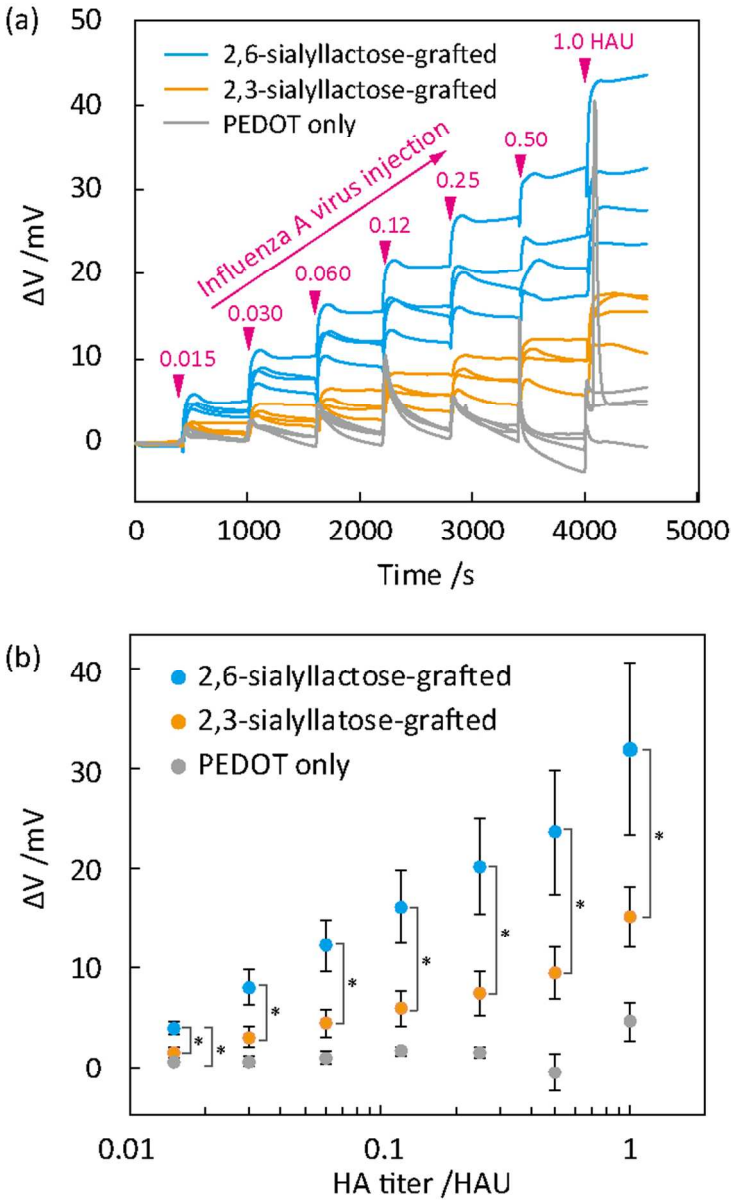

Figure 7. Potentiometric detection of human influenza A virus (H1N1). (a) Time course of the potential change during sequential injection of the human influenza A virus solutions with different HAU (final concentrations: 0, 0.015, 0.03, 0.06, 0.12, 0.25, 0.5 and 1 HAU) in 0.01× DPBS on a 2,6-sialyllactose- or 2,3-sialyllactose-grafted poly(EDOT-co-EDOTOA) film. The electrodes modified with PEDOT only were used as a control. (b) The potential change (ΔV) as a function of human influenza A virus concentrations for each film. Mean ± SD (n = 4). *p < 0.05.

Figure 7
63x104mm (300 x 300 DPI)

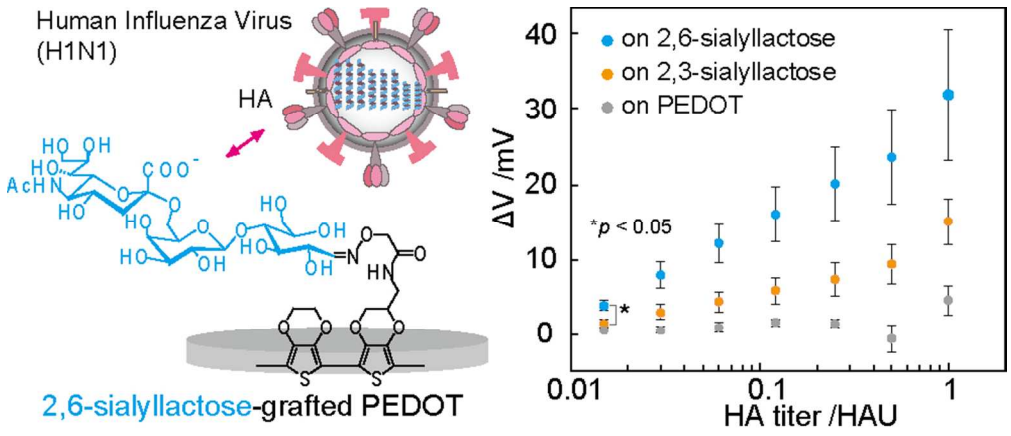

TOC graphic

83x35mm (300 x 300 DPI)